The Namibian Passive Volcanic Margin

Investigations of the South Atlantic Opening with Magnetotelluric and Gravity Data

Gesa Franz[1], Dr. Marion Jegen[1], Dr. Anna Avdeeva[2,3], Dr. Max Moorkamp[2]

[1] Geomar, Helmholtz Centre for Ocean Research, Kiel, Germany
[2] Department of Geology, University of Leicester, UK
[3] Complete MT Solutions Inc., Canada

GEOMAR

Introduction

The source of the magmatic features along the Namibian continental margin and therefore the processes, which lead to the opening of the South Atlantic ocean, are still controversially debated in the literature (Fromm et al., 2017; Bauer et al., 2000; Fairhead & Wilson, 2005) . One big question is weather hotspot volcanism was fed by a deep reaching plume or by heterogeneities of the middle and upper mantle.

In an attempt to gain a better understanding of the involved magmatic processes, we conducted a 3D inversion of magnetotelluric data (Jegen et al., 2016). To improve previous inversion results, a seismically constrained density model (fig. 1) was integrated as a constraint. Inversion was conducted using the jif3D framework (Moorkamp et al., 2011)

The MT data was acquired during cruises MSM 17-1 and -2 (11/2010 – 01/2011). OBEM stations were set out at 45 locations along two perpendicular profiles along and across Walvis ridge (fig. 2) and complemented with data from 8 onshore stations by GFZ Potsdam (Kapinos et al., 2016).

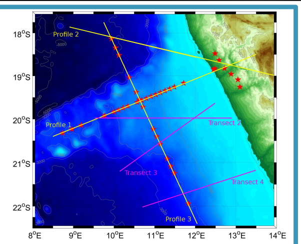

3D Constrained inversion

- Model size: 960 x 960 x 300 km
- Objective function $\Phi(m) = \Phi_d(m) + \lambda \cdot \Phi_{Reg}(m) + \kappa \cdot \Phi_{Cross}(m)$
  - data misfit: $\Phi_d(m) = [g(m) - d_{obs}]^T C_d^{-1} [g(m) - d_{obs}]$
  - regularization misfit: $\Phi_{Reg}(m) = \sum_i \alpha_i m^T W_i^T C_M^{-1} W_i m$
  - Cross gradient coupling: $\Phi_{Cross}(m) = (\nabla m_{res} \times \nabla m_{dens})^T C_M^{-1} (\nabla m_{res} \times \nabla m_{dens})$

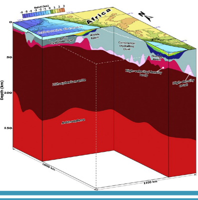

Figure 1 (left): 3D Cube of the density model used as constraint in 3D MT inversion. Figure by Maystrenko et al. (2013).

Figure 2 (above): OBEM locations (red stars) at the Namibian continental margin. Yellow lines are profiles from seismic survey carried out simultaneously to MT measurements . Profile 1 is interpreted by Fromm et al. (2017), Profile 2 and Profile 3 are interpreted by Planert et al. (2016) . Magenta lines are profiles interpreted by Gladczenko et al. (1998)

Cross Gradient Constraint Evaluation

Influence of the starting model

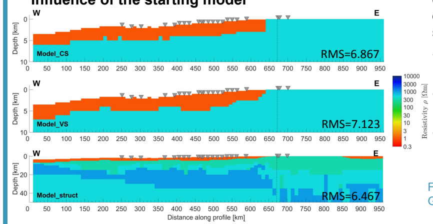

Figure 3 (left): Sections through the three starting models along profile 1. Grey triangles mark MT station locations, dashed line is the coastline

Previous analysis showed that inclusion of a sediment layer is crucial for inversion convergence. We now tested the influence of a constrained sediment thickness and constrained deeper structures in the starting model (figure 3):

- **starting model VS:** constant sediment thickness 3 km (1 Ωm) with 500 Ωm halfspace underneath
- **starting model CS:** sediment thickness retrieved from density model (1 Ωm) with 500 Ωm halfspace underneath
- **starting model struct:** structurally equals the density (constraint-) model

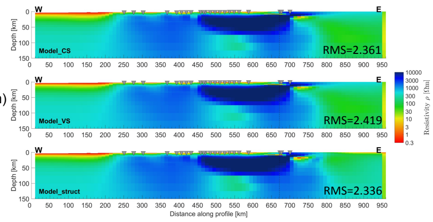

Figure 4 (above): Sections through the resulting 3D models along profile 1 with the different starting models implemented.

Influence of inversion parameters λ and κ

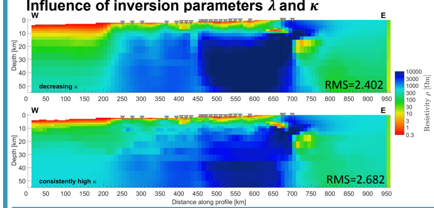

Finding the right strategies for setting the misfit weights λ and κ is crucial for the constrained inversion.

The strategy for the **regularization weight** λ is to start with high values (smooth model) to recover large scale structures in the inversion model first, and then successively decreasing it to enable the development of small scale structures.

For the strategy for the **cross gradient weight** κ, two approaches were tested:

a) **decreasing** κ: the ratio λ/κ is kept relatively constant (from $5 \cdot 10^{-3}$ to $5 \cdot 10^{-2}$) while λ is reduced with increasing number of iterations. This implicates, that parameter κ is reduced simultaneously with λ.

b) **consistently high** κ: the parameter κ is kept high while λ is reduced with increasing number of iterations. This implicates, that the ratio λ/κ decreases with decreasing λ.

Figure 5 (left): Sections through the resulting 3D models along profile 1 of the constrained inversion after approach a) with a decreasing cross gradient weight κ (top) and approach b) with a consistently high κ (bottom)

- inversion is independent of the three tested starting models / inversion was not improved by further constraints in the starting model (figure 4)
- if cross gradient weight κ is chosen too high, model becomes erratic / regularization does not work well anymore (figure 5)

- general benefits of the constrained inversion are:
  1. enhancement of resistivity structures
  2. additional information in areas, where MT data is sparse
  3. no overprint of resistivity data / constraint is not enforced, if one of the models is constant

Geological Results and Conclusion

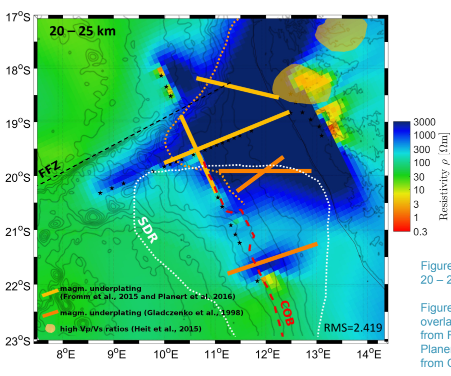

- good correlation of the horizontal extent of the magmatic underplating below seismic profiles (fig. 6 and 7)
- constrain on depth and thickness of magmatic underplating is difficult (fig. 7)
- the Florianopolis fracture zone (FFZ) is imaged clearly in the resistivity model as a boundary to the underplating (fig. 6)
- seaward dipping reflectors (SDR) could not be imaged with the MT data, but underplating terminates at roughly the same areas as SDR begin (continent-ocean-boundary, COB) (fig 6 and fig. 7, bottom)

Figure 6 (left): Horizontal slice through the resulting inversion model at 20 – 25 km overlaid with geological features.

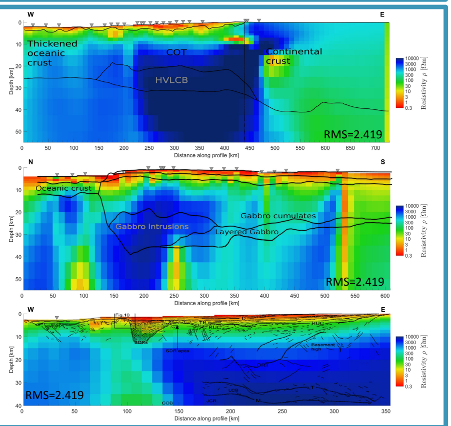

Figure 7 (right): Vertical slices through the resulting model with overlays of seismic interpretations. Profile 1 (top) with interpretations from Fromm et al. (2017), Profile 3 (middle) with interpretations from Planert et al. (2016) and Transect 2 (bottom) with seismic line drawings from Gladczenko et al. (1998)

References

Bauer, K., Neben, S., Schreckenberger, B., Emmermann, R., Hinz, K., Fechner, N., Gohl, K., Schulze, A., Trumbull, R. B., & Weber, K. (2000). Deep structure of the Namibia continental margin as derived from integrated geophysical studies. *Journal of Geophysical Research: Solid Earth*, 105(B11), 25829-25853.
Fairhead, J. D., & Wilson, M. (2005). Plate tectonic processes in the South Atlantic Ocean: do we need deep mantle plumes?. *Geological Society of America Special Papers*, 388, 537-553.
Fromm, T., Jokat, W., Ryberg, T., Behrmann, J. H., Haberland, C., & Weber, M. (2017). The onset of walvis ridge: Plume influence at the continental margin. *Tectonophysics*.
Kapinos, G., Weckmann, U., Jegen-Kulcsar, M., Meqbel, N., Neska, A., Katjiuongua, T., Hölz, S., & Ritter, O. (2016). Electrical resistivity image of the South Atlantic continental margin derived from onshore and offshore magnetotelluric data. *Geophysical Research Letters*, 43(1), 154-160.
Jegen, M., Avdeeva, A., Berndt, C., Franz, G., Heincke, B., Hölz, S., Neska, A., Marti, A., Planert, L., Kopp, H., Baba, K., Ritter, O., Weckmann, U., Meqbel, N., & Behrmann, J. (2016). 3-D magnetotelluric image of offshore magmatism at the Walvis Ridge and rift basin. *Tectonophysics*, 683, 98-108.
Maystrenko, Y. P., Scheck-Wenderoth, M., Hartwig, A., Anka, Z., Watts, A. B., Hirsch, K. K., & Fishwick, S. (2013). Structural features of the Southwest African continental margin according to results of lithosphere-scale 3D gravity and thermal modelling. *Tectonophysics*, 604, 104-121.
Moorkamp, M., Heincke, B., Jegen, M., Roberts, A. W., & Hobbs, R. W. (2011). A framework for 3-D joint inversion of MT, gravity and seismic refraction data. *Geophysical Journal International,* 184(1), 477-493.
Planert, L., Behrmann, J., Jokat, W., Fromm, T., Ryberg, T., Weber, M., & Haberland, C. (2016). The wide-angle seismic image of a complex rifted margin, offshore north namibia: Implications for the tectonics of continental breakup. *Tectonophysics*.

HELMHOLTZ GEMEINSCHAFT